Resonant nuclear reaction ^{23}Mg (p,γ) ^{24}Al in strongly screening magnetized neutron star crust *

Jing-Jing Liu(刘晶晶)[1)] Dong-Mei Liu(刘冬梅)[2)]

College of Marine Science and Technology, Hainan Tropical Ocean University, Sanya, Hainan 572022, China

Abstract: Based on the relativistic theory of superstrong magnetic fields (SMF), by using three models those of Lai (LD), Fushiki (FGP), and our own (LJ), we investigate the influence of SMFs due to strong electron screening (SES) on the nuclear reaction ^{23}Mg (p,γ) ^{24}Al in magnetars. In a relatively low density environment (e.g., $\rho_7<0.01$) and $1<B_{12}<10^2$, our screening rates are in good agreement with those of LD and FGP. However, in relatively high magnetic fields (e.g., $B_{12}>10^2$), our reaction rates can be 1.58 times and about three orders of magnitude larger than those of FGP and LD, respectively (B_{12}, ρ_7 are in units of 10^{12}G, 10^7g cm^{-3}). The significant increase of strong screening rate can imply that more ^{23}Mg will escape from the Ne-Na cycle due to SES in a SMF. As a consequence, the next reaction, ^{24}Al (β^+,ν) ^{24}Mg, will produce more ^{24}Mg to participate in the Mg-Al cycle. Thus, it may lead to synthesis of a large amount of $A>20$ nuclides in magnetars.

Keywords: dense matter: nuclear reactions, nucleosynthesis, abundances, stars: magnetic fields, stars: magnetars

PACS: 24.30.-v, 26.20.Np, 26.60.Gj **DOI:** 10.1088/1674-1137/41/12/125102

1 Introduction

In the dense sites of the universe, such as novae, X-ray bursts and supernovae, there are explosive hydrogen burning processes in high temperature and high hydrogen environments. This burning is called the rapid-proton (rp) process [1]. In the stage of hydrogen burning, proton capture reactions and β^+-decays (rp-process) will be ignited in nuclei with mass number $A>20$. For example, the timescale of the proton capture reaction of ^{23}Mg in the Ne-Na cycle at sufficiently high temperature is shorter than that of β^+-decay. Therefore, some ^{23}Mg will kindle and escape from the Ne-Na cycle by proton capture. The ^{23}Mg leaks from the Ne-Na cycle into the Mg-Al cycle, synthesizing a large amount of heavy nuclei. Thus the reaction ^{23}Mg (p,γ) ^{24}Al in stellar environments is an important reaction for producing heavy nuclei. Wallace et al. [1] first discussed the reaction rate of ^{23}Mg (p,γ) ^{24}Al. Then, Iliadis et al. [2] also investigated this nuclear reaction rate. Kubono et al. [3] reconsidered the rate by considering four resonances and the structure of ^{24}Al. Based on some new experimental information on ^{24}Al excitation energies, Herndl et al. [4], Visser et al. [5], carried out an estimation of the rate. However, they all seem to have overlooked the influence of electron screening on nuclear reactions.

In pre-supernova stellar evolution and nucleosynthesis, strong electron screening (SES) is always a challenging and interesting problem. Some works [6–12] have been done on stellar weak-interaction rates and thermonuclear reaction rates. Some SES models for high-density environments have been widely investigated, including the Salpeter model [13, 14], Graboske model [15], and Dewitt model [16]. Recently these issues were discussed by Liolios et al. [17, 18], and Liu [8]. However, they neglected the effects of SES on thermonuclear reaction rate in superstrong magnetic fields (SMF).

It is widely known that nuclear reaction rates at low energies play a key role in energy generation in stars and in stellar nucleosynthesis. The bare reaction rates are modified in stars by the screening effects of free and bound electrons. Knowledge of the bare nuclear reaction rates at low energies is important not only to understand various astrophysical nuclear problems, but also to assess the effects of host material in low energy nuclear fusion reactions in matter.

It is generally accepted that the surface dipole magnetic field strengths of magnetars are in a range from 10^{13}

Received 30 March 2017, Revised 26 September 2017

∗ Supported by National Natural Science Foundation of China (11565020), the Counterpart Foundation of Sanya (2016PT43), the Special Foundation of Science and Technology Cooperation for Advanced Academy and Regional of Sanya (2016YD28), the Scientific Research Starting Foundation for 515 Talented Project of Hainan Tropical Ocean University (RHDRC201701) and the Natural Science Foundation of Hainan Province (114012)

1) E-mail: syjjliu68@qzu.edu.cn

2) E-mail: liudongmei72@126.com

to 10^{15} G [19–27]. The momentum space of the electron gas is modified substantially by such intense magnetic fields. The electron Fermi energy and nuclear reactions are also greatly affected by SMFs in magnetars.

Anomalous X-ray pulsars (AXPs) and soft gamma-ray repeaters (SGRs) are conceived as magnetars, which are a special kind of pulsar powered by their magnetic energy [28]. The Fermi energy of the electrons will increase with magnetic field, and the quantum effects of the electron gas will be very obvious in a SMF. As we know, the positive energy levels of electrons must abide by Landau quantization. The distribution of electrons in momentum space will be strongly modified by a SMF. Some authors have discussed this issue in detail for the strong magnetic fields of magnetars. For instance, Gao et al. [23, 24, 25] investigated not only the spin-down and magnetic field evolutions, but also the electron Landau level effects on emission properties of magnetars.

In this paper, based on relativistic theory in a SMF [20–23, 25], we discuss the problem of SES and then investigate the effect of SES on the thermonuclear reaction on the surface of magnetars within three different models (i.e., our model (LJ), Lai's model (LD) [27, 29], and Fushiki's model (FGP) [30]).

This work differs from our previous work [10] on the discussion of nuclear reaction rates. Firstly, in Ref. [10], though we cited several works from Gao et al., we were not familiar with the calculations involved in electron Fermi energy in a superhigh magnetic field, so a non-relativistic electron cyclotron solution was applied when calculating the rates. Secondly, Ref. [10] did not compare the LJ, LD, and FGP models in the case with a SMF. Finally, we analyze the nuclear reaction rates in a SMF and also compare our model with the Dewitt model [16], and Liolios model [17], in which SMFs were not taken into consideration. Maybe SES universally occurs in pulsars, and the screening rate calculations in SMFs are important for future studies on cooling, nucleosynthesis, and emission properties of magnetars.

In this paper, following the works of Peng et al. [20], and Gao et al. [21, 22, 23, 25], we calculate the resonant reaction rates in the case with SMF and without SMF in several screening models. In the case of the former, the results from the LD and FGP models will be compared with those of our model, while in the latter case, the results from the Dewitt and Liolios models also will be compared. We derive new results for SES theory and the screening rates for nuclear reactions in relativistic strong magnetic fields.

The article is organized as follows. In the next section, we analyse three SES models for a SMF in magnetars. In Section 3 we discuss the effects of SES on the proton capture reaction rate of ^{23}Mg, in which the four resonances contributions will also be considered. The results and discussions will be shown in Section 4. The article is closed with some conclusions in Section 5.

2 SES in a SMF

In astrophysical systems, the SMF may have significant influence on the quantum processes. In this section, we will study three models of the electron screening potential (ESP) in a SMF, i.e., the LJ model, LD model, and FGP model.

2.1 ESP in our model

The rate of nuclear reactions in high density matter is affected by how the clouds of electrons surrounding the nuclei alter the interactions among nuclei. The positive energy levels of electrons in a SMF are given by [31]

$$\frac{\varepsilon_n}{m_{\rm e}c^2}=\left[\left(\frac{p_{\rm z}}{m_{\rm e}c}\right)+1+2\left(n+\frac{1}{2}+\sigma\right)b\right]^{1/2}=(p_z^2+\Theta)^{1/2}, \quad (1)$$

where $\Theta=1+2(n+\frac{1}{2}+\sigma)b$, $n=0,1,2,3....$, $b=\frac{B}{B_{\rm cr}}=0.02266B_{12}$, B_{12} is the magnetic field in units of 10^{12} G, i.e., $B_{12}\equiv B/10^{12}$ G, $B_{\rm cr}=\frac{m_{\rm e}^2c^3}{e\hbar}=4.414\times10^3$ G is the electron quantum critical magnetic field, p_z is the electron momentum along the field, and σ is the spin quantum number of an electron, when $n=0$, $\sigma=1/2$, and when $n\geq1$, $\sigma=\pm1/2$.

In an extremely strong magnetic field ($B\gg B_{\rm cr}$), the Landau column becomes a very long and narrow cylinder along the magnetic field. According to the Pauli exclusion principle, the electron number density should be equal to its microscopic state density. By introducing the electron Landau level stability coefficient, the Fermi energy of the electron is given by [22, 32]

$$\begin{aligned}U_{\rm F} &= 5.91\times10^4\left(\frac{B}{B_{\rm cr}}\right)^{1/6}\left(\frac{\rho Y_{\rm e}}{\rho_0\times0.00564}\right)^{1/3}\\ &= 5.91\times10^4\left(\frac{B}{B_{\rm cr}}\right)^{1/6}\left(\frac{n_{\rm e}}{0.00564\times\rho_0N_{\rm A}}\right)^{1/3}\ {\rm keV}, \quad (2)\end{aligned}$$

where $\rho_0=2.8\times10^{14}{\rm g/cm}^3$ is the standard nuclear density.

In order to evaluate the Thomas-Fermi screening wave-number $K_{\rm TF}^{\rm LJ}$, we define a parameter $D^{\rm LJ}(U_{\rm e})$ and then, from Eq. (2), we have

$$n_{\rm e}=0.00564\rho_0N_{\rm A}\left(\frac{U_{\rm F}}{5.91\times10^4b^{1/6}}\right)^3 \quad (3)$$

$$\begin{aligned}D^{\rm LJ}(U_{\rm F}) &= \frac{\partial n_{\rm e}}{\partial U_{\rm F}}=\frac{\partial}{\partial U_{\rm F}}\left(0.00564\rho_0N_{\rm A}\left(\frac{U_{\rm F}}{5.910\times10^4b^{1/6}}\right)^3\right)\\ &= 4.9913\times10^7n_{\rm e}^{2/3}b^{-1/6}\quad {\rm cm^{-3}\ KeV^{-1}}. \quad (4)\end{aligned}$$

The Thomas-Fermi screening wave-number $K_{\rm TF}^{\rm LJ}$ is

then given by [33]

$$(K_{\rm TF}^{\rm LJ})^2 = 4\pi e^2 D^{\rm LJ}(U_{\rm F})=4\pi e^2\frac{\partial n_{\rm e}}{\partial U_{\rm F}} = 6.269\times10^7 e^2(n_{\rm e})^{2/3}b^{-1/6} \quad {\rm cm}^{-3}. \quad (5)$$

By using the uniform electron gas model [34], the binding energy of the magnetized condensed matter at zero pressure can be estimated. The energy per cell can be written as

$$E_{\rm total}=E_{\rm k}+E_{\rm latt}=\frac{3\pi^2e^2z_j^3}{8b_1^2r_i^6}+\frac{9e^2z^{\frac{5}{3}}}{10r_{\rm e}} \quad {\rm MeV}, \quad (6)$$

where the first term is the kinetic energy and the second term is the lattice energy. $r_i=z^{1/3}r_{\rm e}a_0$ is the Wigner-Seitz cell radius, $a_0=0.529\times10^{-8}$cm is the Bohr radius, and $r_{\rm e}=(3/4\pi n_{\rm e})^{1/3}$ is the mean electron spacing. z_j is the charge number of species j. $b_1=B/B_0=425.4B_{12}=1.9773\times10^4b$ and $B_0=m_{\rm e}^2ce^3/\hbar^3=2.3505\times10^{-9}$ G is the natural (atomic) unit for the field strength [27]. For zero-pressure condensed matter, we require ${\rm d}E_{\rm total}/{\rm d}r_i=0$, so we have

$$r_i=r_{i0}=0.0371z_j^{1/5}b^{-2/5}a_0 \quad {\rm cm}. \quad (7)$$

By using linear response theory, the energy correction per cell due to non-uniformity is given by [35]

$$E_{\rm TF}^{\rm LJ}(r_i,z_j) = -\frac{18}{175}(K_{\rm TF}^{\rm LJ}r_i)^2\frac{(z_je)^2}{r_i} = -\frac{1.30\times10^{-6}e^6(n_{\rm e})^{4/3}z_j^{9/5}}{b^{11/15}} \quad {\rm MeV}. \quad (8)$$

For relativistic electrons, the influence from exchange free energy was discussed in Refs. [36, 37]. Their work showed that the correlation correction is very small. Therefore, in this paper we have neglected the correction of the Coulomb exchange free energy interaction in the electron gas model. By taking into consideration the Coulomb energy and Thomas-Fermi correction due to non-uniformity of the electron gas, the energy per cell should be corrected as

$$E_{\rm s}^{\rm LJ}(r_i,z_j)=E_{\rm k}(r_i,z_j)-U_{\rm coul}(r_i,z_j)-E_{\rm TF}^{\rm LJ}(r_i,z_j). \quad (9)$$

For two interaction nuclides, the energy required to bring two nuclei with nuclear charge numbers z_1 and z_2 so close together that they essentially coincide differs from the bare Coulomb energy by an amount which in the Wigner-Seitz approximation is

$$U_{\rm sc}=E_{\rm s}(r_i,z_{12})-E_{\rm s}(r_i,z_1)-E_{\rm s}(r_i,z_2), \quad (10)$$

where $z_{12}=z_1+z_2$. If the electron distribution is rigid, the contributions to $E_{\rm s}$ from the bulk electron energy cancel, and the screening potential is simply given as

$$U_{\rm sc} = E_{\rm coul}(r_i,z_{12})-E_{\rm coul}(r_i,z_1)-E_{\rm coul}(r_i,z_2) = 6.5984\times10^4b^{2/5}(z_{12}^{9/5}-z_1^{9/5}-z_2^{9/5}){\rm MeV}, \quad (11)$$

where we assume the electron density is uniform, and the screening potential is independent of the magnetic field.

From Eq. (9), the change in the screening potential due to the compressibility of electrons in zero-pressure magnetized condensed matter can obtained as

$$\delta E_{\rm TF}^{\rm LJ} = -\frac{18}{175}(K_{\rm TF}^{\rm LJ}r_i)^2\frac{e^2(z_{12}^2-z_1^2-z_2^2)}{r_i} = -\frac{1.30\times10^{-6}e^6n_{\rm e}^{4/3}(z_{12}^{9/5}-z_1^{9/5}-z_2^{9/5})}{b^{11/15}}. \quad (12)$$

In accordance with the above discussions, the total screening potential is the sum of the screening potential with a uniform distribution and a corrected screening potential with a non-uniform distribution. The screening potential in a SMF is given by

$$U_{\rm sc}^{\rm LJ}=U_{\rm sc}+\delta E_{\rm TF}^{\rm LJ}. \quad (13)$$

2.2 ESP in LD model

Refs. [27] and [29] discussed the equation of state and the electron energy in a SMF. In a SMF, the electron number density $n_{\rm e}$ is related to the chemical potential $U_{\rm e}$ by

$$n_{\rm e} = \frac{1}{(2\pi\widehat{\rho})^2\hbar}\sum_0^\infty g_{n0}\int_{-\infty}^{+\infty}f{\rm d}p_z = \frac{1}{(2\pi\widehat{\rho})^2\hbar}\sum_0^\infty g_{n0}\int_{-\infty}^{+\infty}\left[1+\exp\left(\frac{E-U_{\rm e}}{kT}\right)\right]^{-1}{\rm d}p_z, \quad (14)$$

where $\widehat{\rho}=(\hbar c/eB)^{1/2}=2.5656\times10^{-10}B_{12}^{1/2}$cm is the electron cyclotron radius (the characteristic size of the wave packet), $E=[c^2p_z^2+m_{\rm e}c^4(1+nb)]^{1/2}$ is the free electron energy, g_n is the spin degeneracy of the Landau level, $g_{00}=1$ and $g_{n0}=2$ for $n\geqslant1$, and the Fermi-Dirac distribution is given by

$$f=\left[1+\exp\left(\frac{E-U_{\rm e}}{kT}\right)\right]^{-1}. \quad (15)$$

The electron Fermi energy including the electron rest mass is given by

$$n_{\rm e}=\frac{1}{2\pi^{3/2}\lambda_{\rm Te}\widehat{\rho}^2}\sum_{(n=0)}^\infty g_nI_{-1/2}\left(\frac{U_{\rm e}-n\hbar\omega_{\rm ce}}{kT}\right), \quad (16)$$

where the thermal wavelength of the electron is $\lambda_{\rm Te}=(2\pi\hbar^2/m_{\rm e}kT)^2$, and the Fermi integral is written as

$$I_n(y)=\int_0^\infty\frac{x^n}{\exp(x-y)+1}{\rm d}x. \quad (17)$$

The binding energy of magnetized condensed matter at zero pressure can be estimated using the uniform electron gas model. Under the condition of a super-strong magnetic field, the Fermi energy $U_{\rm F}$ is less than the cyclotron energy $\hbar\omega_{\rm ce}$, and the electrons only occupy the ground Landau level. According to Ref. [27], the

Thomas-Fermi screening wave-number is given by

$$(K_{\rm TF}^{\rm LD})^2=4\pi e^2 D^{\rm LD}(\varepsilon_{\rm F})=4\pi e^2\frac{\partial n_{\rm e}}{\partial\varepsilon_{\rm F}}=4\pi e^2\frac{\partial n_{\rm e}}{\partial U_{\rm F}}, \quad (18)$$

where $\partial n_{\rm e}/\partial\varepsilon_{\rm F}$ is the density of states per unit volume at the Fermi surface. $\varepsilon_{\rm F}=P_{\rm F}^2/2m_{\rm e}$. From Eq. (6.16) of Ref. [27], we have

$$D^{\rm LD}=\frac{\partial n_{\rm e}}{\partial\varepsilon_{\rm F}}=\frac{3.79\times10^6 b^2 r_{\rm e}^3}{e^2}. \quad (19)$$

The Thomas-Fermi screening wave-number is given by

$$K_{\rm TF}^{\rm LD}=(\frac{4}{3\pi^2})^{1/2}b_1 r_{\rm e}^{3/2}=6.901\times10^3 b r_{\rm e}^{3/2}. \quad (20)$$

Using the linear response theory, the energy correction (in atomic units) per cell due to non-uniformity can be calculated and given by [27]

$$E_{\rm TF}^{\rm LD}(r_i,z_j)=-\frac{18}{175}(K_{\rm TF}^{\rm LD}r_i)^2\frac{e^2 z_j^2}{r_i}=-0.0139 b_1^2 r_i^4 z_j. \quad (21)$$

The uniform electron gas model can be improved by taking into consideration the Coulomb energy and Thomas-Fermi correction due to non-uniformity of the electron gas. When the electron density is assumed to be uniform, the screening potential is independent of the magnetic field. The change of the screening potential due to the compressibility of the electrons for zero-pressure magnetized condensed matter can obtained as

$$\delta E_{\rm TF}^{\rm LD}=-2.5236\times10^{-4}b^{2/5}(z_{12}^{9/5}-z_1^{9/5}-z_2^{9/5}). \quad (22)$$

When we sum a screening potential with a uniform distribution and a corrected screening potential with a non-uniform distribution, the screening potential in a SMF is given by

$$U_{\rm s}^{\rm LD}=U_{\rm sc}+\delta E_{\rm TF}^{\rm LD}. \quad (23)$$

2.3 ESP in FGP model

The influence of SES in a SMF on nuclear reactions was also discussed in detail by Fushiki et al. [30] (FGP). The electron Coulomb energy in the Wigner-Seitz approximation in a SMF was given by

$$U_{\rm sc}^{\rm FGP}=E_{\rm atm}(r_i,z_{12})-E_{\rm atm}(r_i,z_1)-E_{\rm atm}(r_i,z_2), \quad (24)$$

where $E_{\rm atm}(r_i,z_j)$ is the total energy of Wigner-Seitz cell. If the electron distribution is rigid, the contributions to $E_{\rm atm}(r_i,z_j)$ from the bulk electron energy cancel, and the electron screening potential at high density can be expressed as

$$U_{\rm sc}^{\rm FGP}=E_{\rm latt}(r_i,z_{12})-E_{\rm latt}(r_i,z_1)-E_{\rm latt}(r_i,z_2), \quad (25)$$

where $E_{\rm latt}(r_i,z_j)$ is the electrostatic energy of a Wigner-Seitz cell and $E_{\rm atm}(r_i,z_j)=-0.9z_j^{5/3}e^2/r_{\rm e}$. Due to the compressibility of the electron, the change in the screening potential is given by [30]

$$\begin{aligned}\delta U_{\rm s}^{\rm FGP} &= -\frac{54}{175}\left(\frac{e^2}{r_{\rm e}}\right)\frac{1}{n_{\rm e}}\frac{\partial n_{\rm e}}{\partial U_{\rm e}}[(z_{12})^{7/3}-(z_1)^{7/3}-(z_2)^{7/3}]\\ &= -\frac{54}{175}\left(\frac{e^2}{r_{\rm e}}\right)\frac{1}{n_{\rm e}}D^{\rm FGP}[(z_{12})^{7/3}-(z_1)^{7/3}-(z_2)^{7/3}],\end{aligned} \quad (26)$$

where

$$D^{\rm FGP}=823.1481\frac{r_{\rm e}n_{\rm e}}{e^2}\left(\frac{\overline{A}}{z}\right)^{4/3}\rho^{-4/3}B_{12}^2. \quad (27)$$

The Thomas-Fermi screening wave-number is given by

$$(K_{\rm TF}^{\rm FGP})^2=1.0344\times10^4 r_{\rm e}n_{\rm e}\left(\frac{\overline{A}}{z}\right)^{4/3}\rho^{-4/3}B_{12}^2. \quad (28)$$

Thus, the corresponding result for the changes in the screening potential in a SMF is

$$\delta U_{\rm s}^{\rm FGP}=-0.254\left(\frac{\overline{A}}{z}\right)^{4/3}\rho^{-4/3}B_{12}^2[(z_{12})^{7/3}-(z_1)^{7/3}-(z_2)^{7/3}]=-494.668\left(\frac{\overline{A}}{z}\right)^{4/3}\rho^{-4/3}b^2[(z_{12})^{7/3}-(z_1)^{7/3}-(z_2)^{7/3}]\ {\rm MeV}, \quad (29)$$

where $(\overline{A/z})$ is the average ratio of A/z, which corresponds to the mean molecular weight per electron. Thus, the electron screening potential in a SMF in the FGP model is given by

$$U_{\rm s}^{\rm FGP}=U_{\rm sc}+\delta E_{\rm TF}^{\rm FGP}=U_{\rm sc}+\delta U_{\rm s}^{\rm FGP}. \quad (30)$$

3 Resonant reaction process and rates

3.1 Calculations of resonant reaction rates with and without SES

The reaction rates are the sums of contributions from the resonant and non-resonant reactions. In the case of a narrow resonance, the resonant cross section $\sigma_{\rm r}$ is approximated by a Breit-Wigner expression [38]

$$\sigma_{\rm r}(E)=\frac{\pi\omega}{\kappa^2}\frac{\Lambda_{\rm i}(E)\Lambda_{\rm f}(E)}{(E-E_{\rm r}^2)+\frac{\Lambda_{\rm total}^2(E)}{4}}, \quad (31)$$

where κ is the wave number, and the entrance and exit channel partial widths are $\Lambda_{\rm i}(E)$ and $\Lambda_{\rm f}(E)$, respectively. $\Lambda_{\rm total}(E)$ is the total width, and the statistical factor, ω, is given by

$$\omega=(1+\delta_{12})\frac{2J+1}{(2J_1+1)(2J_2+1)}, \quad (32)$$

where the spins of the interacting nuclei and the resonance are J_1, and J_2, respectively, and δ_{12} is the Kronecker delta.

The partial widths are dependent on the energy, and can be written as [39]

$$\Lambda_{\rm i,f}=2\vartheta^2_{\rm i,f}\psi_l(E,a)=\Lambda_{\rm i,f}\frac{\psi_l(E,a)}{\psi_l(E_{\rm f},a)}. \quad (33)$$

The penetration factor ψ_l is associated with l and a, which are the relative angular momentum and the channel radius, respectively. $a=1.4(A_1^{1/3}+A_2^{1/3})$ fm. $\Lambda_{\rm i,f}$ is the partial energy width at the resonance process. $E_{\rm r}$ and $\vartheta^2_{\rm i,f}$ are the reduced widths, given by

$$\vartheta^2_{\rm i,f}=0.01\vartheta^2_{\rm w}=\frac{0.03\hbar^2}{2Aa^2}. \quad (34)$$

Based on the above analysis, in the explosive stellar burning phase, the narrow resonance reaction rates without SES are determined by [4, 40]

$$\lambda^0_{\rm r} = N_{\rm A}\langle\sigma v\rangle_{\rm r}=1.54\times10^{11}(AT_9)^{-3/2} \times\sum_i\omega\gamma_i\exp(-11.605E_{{\rm r}_i}/T_9) \quad {\rm cm^3mol^{-1}s^{-1}}, \quad (35)$$

where $N_{\rm A}$ is Avogadro's constant, A is the reduced mass of the two collision partners, $E_{{\rm r}_i}$ is the resonance energies and T_9 is the temperature in units of 10^9 K. The $\omega\gamma_i$ is the strength of the resonance in units of MeV and is given by

$$\omega\gamma_i=(1+\delta_{12})\frac{2J+1}{(2J_1+1)(2J_2+1)}\frac{\Lambda_{\rm i}\Lambda_{\rm f}}{\Lambda_{\rm total}}. \quad (36)$$

The reaction rates of narrow resonances with SES are given by

$$\begin{aligned}\lambda^s_{\rm r} &= F_{\rm r}N_{\rm A}\langle\sigma v\rangle_{\rm r'}\\ &= 1.54\times10^{11}(AT_9)^{-3/2}\sum_i\omega\gamma_i\exp(-11.605E^{'}_{{\rm r}_i}/T_9)\\ &= 1.54\times10^{11}F_{\rm r}(AT_9)^{-3/2}\\ &\quad\times\sum_i\omega\gamma_i\exp(-11.605E_{{\rm r}_i}/T_9)\ {\rm cm^3mol^{-1}s^{-1}}, \quad (37)\end{aligned}$$

where $F_{\rm r}$ is the screening enhancement factor (SEF). The values of $E^{'}_{{\rm r}_i}$ should be measured by experiment, but it is too hard to provide sufficient data. In a general and approximate analysis, we have $E^{'}_{{\rm r}_i}=E_{{\rm r}_i}-U_0=E_{{\rm r}_i}-U_{\rm s}$.

3.2 Screening model of resonant reaction rates without SMF

3.2.1 Dewitt model

Dewitt et al. [16] discussed the problem of thermonuclear ion-electron screening at some densities. Based on a statistical mechanical theory for the screening function, the influence of electron screening on the nuclear reaction process was also investigated in their paper. The strong electron screening potential function is given by [16]

$$\begin{aligned}H^{\rm sc}_{12} = \frac{e^2}{r_{\rm e}kT}&\{0.9(\overline{z})^{1/3}(z_{12}^{5/3}-z_1^{5/3}-z_2^{5/3})\\ &+c_1(\overline{z})^{2/3}(z_{12}^{4/3}-z_1^{4/3}-z_2^{4/3})\}\\ &+[c_2(\overline{z})^{-2/3}(z_{12}^{2/3}-z_1^{2/3}-z_2^{2/3})], \quad (38)\end{aligned}$$

where $c_1=0.2843$ and $c_2=0.4600$, and $\overline{z}$, the average ionic charge, is given by

$$\overline{z}=\sum_i z_i f_i=\sum_i z_i\frac{n_i}{n_{\rm I}}, \quad (39)$$

where n_i and $n_{\rm I}$ are the ion densities of nuclear species i and I of the total system, respectively.

The screening enhancement factor (SEF) in the Dewitt model is written as

$$F^0_{\rm r}({\rm Dew})=\exp({\rm H}^{\rm sc}_{12}). \quad (40)$$

3.2.2 Liolios model

At astrophysical energies the electron-screening acceleration in laboratory fusion reactions always plays a key role and is an interesting problem for astrophysics. Based on a mean-field model, Liolios et al. [17] studied the screened nuclear reactions at astrophysical energies. The electron screening potential in the Liolios-screened Coulomb model is given as [17]

$$U^{\rm Lios}_0=\frac{15}{8}\frac{z_1z_2e^2}{\Xi}, \quad (41)$$

where

$$\Xi=\left(\frac{15}{8\pi z_i^2}\right)^{1/3}a_0=0.8853a_0(z_1^{2/3}+z_2^{2/3})^{1/2}. \quad (42)$$

The SEF for the resonant reaction in the Liolios model is

$$F^0_{\rm r}({\rm Lios})=\exp\left(\frac{11.605U^{\rm Lios}_0}{T_9}\right). \quad (43)$$

3.3 Screening model of resonant reaction rates in SMFs

In this subsection, we will discuss the screening potential in the strong screening limit. The dimensionless parameter (Γ), which determines whether or not correlations between two species of nuclei (z_1,z_2) are important, is given by

$$\Gamma=\frac{z_1z_2e^2}{(z_1^{1/3}+z_2^{1/3})r_{\rm e}kT}, \quad (44)$$

When $\Gamma\gg1$, the nuclear reaction rates will be influenced appreciably by SES. According to the above three SES models (LD, FGP, LJ) for SMFs, the three enhancement factors for resonant reaction processes in SMFs can be expressed as follows

$$F^{\rm B}_{\rm r}({\rm LD})=\exp\left(\frac{11.605U^{\rm LD}_{\rm s}}{T_9}\right), \quad (45)$$

$$F_{\rm r}^{\rm B}({\rm FGP})=\exp\left(\frac{11.605U_{\rm s}^{\rm FGP}}{T_9}\right), \quad (46)$$

$$F_{\rm r}^{\rm B}({\rm LJ})=\exp\left(\frac{11.605U_{\rm s}^{\rm LJ}}{T_9}\right). \quad (47)$$

4 Numerical results

4.1 Analysis of the results for SEF

Strong magnetic fields significantly modify the properties of matter and always play a critical role in astronomical conditions. Figure 1 presents the variations of ESP as a function of B_{12} for our SES model. The SMF has only a slight influence on ESP when $B_{12}>3\times10^3$ and $\rho_7<1$. However, the ESP increases greatly when $B_{12}<1.4\times10^3$ and $\rho_7<1$ (B_{12}, ρ_7 are in units of 10^{12} G, 10^7g cm^{-3}, respectively). The numerical results in our model show that the maximum value of ESP reaches 0.1 MeV. Figure 2(a) presents the ESP in the LD model as a function of B_{12}. The ESP increases rapidly and reaches a maximum value of 0.008442 MeV at $B_{12}=80$, then decreases with increasing SMF.

Based on the Thomas-Fermi and Thomas-Fermi-Dirac approximations, Fushiki et al. [30] analyzed the electron Fermi energy, electron Landau level, and SES problem in a SMF. Their results show that, as a consequence of the field dependence of the screening potential, magnetic fields can significantly increase nuclear reaction rates [30]. Using the electron screening model of Ref. [30] (the FGP model) in a SMF, Fig. 2(b) shows the ESP as a function of B_{12} under some typical astrophysical conditions. The ESP increases greatly when $B_{12}<10^3$ and gets to a maximum value of 0.0188 MeV at $B_{12}=580.7$ and $\rho_7=0.1$. The ESP then decreases by around two orders of magnitude when $10^3<B_{12}<2\times10^3$ at $\rho_7=0.1$.

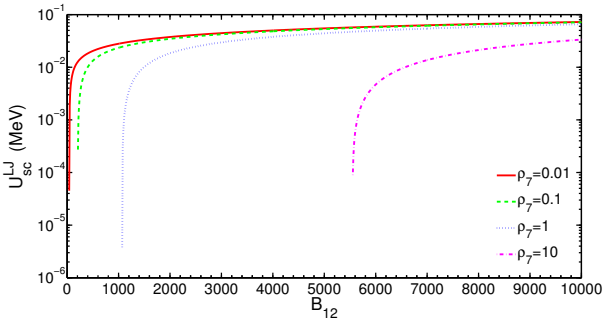

Fig. 1. (color online) The electron screening potential as a function of B_{12} in the LJ model, for some typical astronomical conditions.

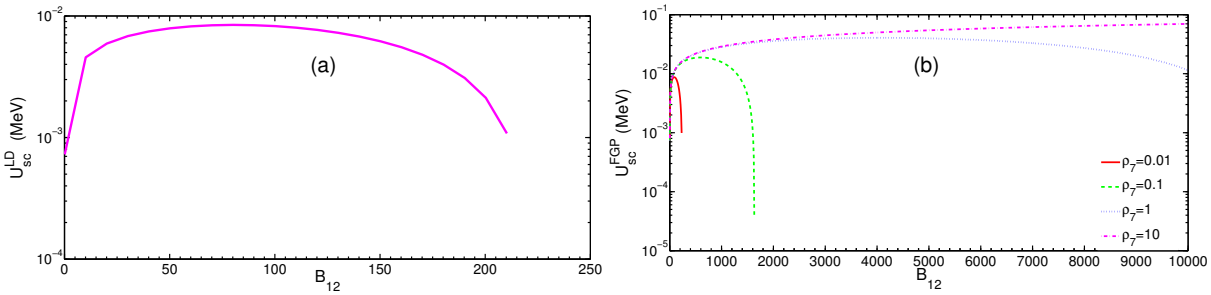

Fig. 2. (color online) The electron screening potential as a function of B_{12} in the LD and FGP models, for some typical astronomical conditions.

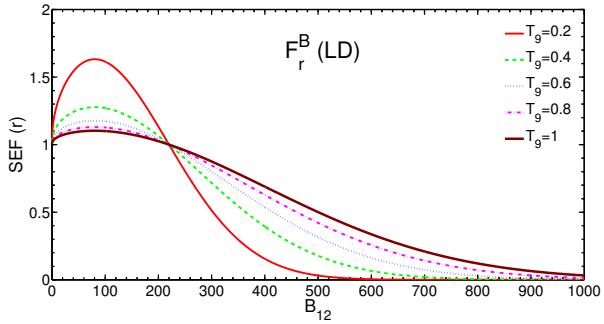

Fig. 3. (color online) The resonant SEF for the LD model as a function of B_{12} in the case with SES and SMF.

The influence of SES in a SMF on nuclear reactions is mainly reflected by the SEF. We discuss the influence of SES on SEF by three models (LD, FGP, LJ) from Fig. 3 to Fig. 4. The SEF of the LD model is a sensitive parameter for SMF and temperature. The maximum value of the SEF is about 1.632 for $B_{12}=78.17$ and $T_9=0.2$, as shown in Fig. 3, where T_9 is the temperature in units of 10^9 K. For $B_{12}>219.3$, however, the SEF is less than 1.001. Figure 4 presents the SEF as a function of B_{12} for the FGP and LJ models. From Fig. 4(a) and 4(b), the shift of SEF in the FGP model is in good agreement with that of the LD model at low density (e.g. $\rho_7=0.01$). The maximum value of SEF for the FGP model is about

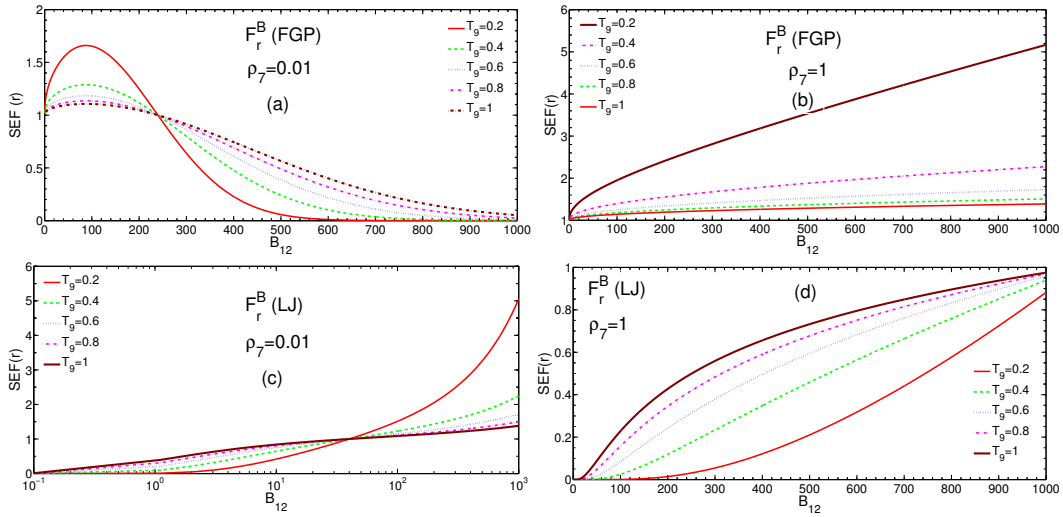

Fig. 4. (color online) The resonant SEF for the FGP and LJ models as a function of B_{12} in the case with SES and SMF.

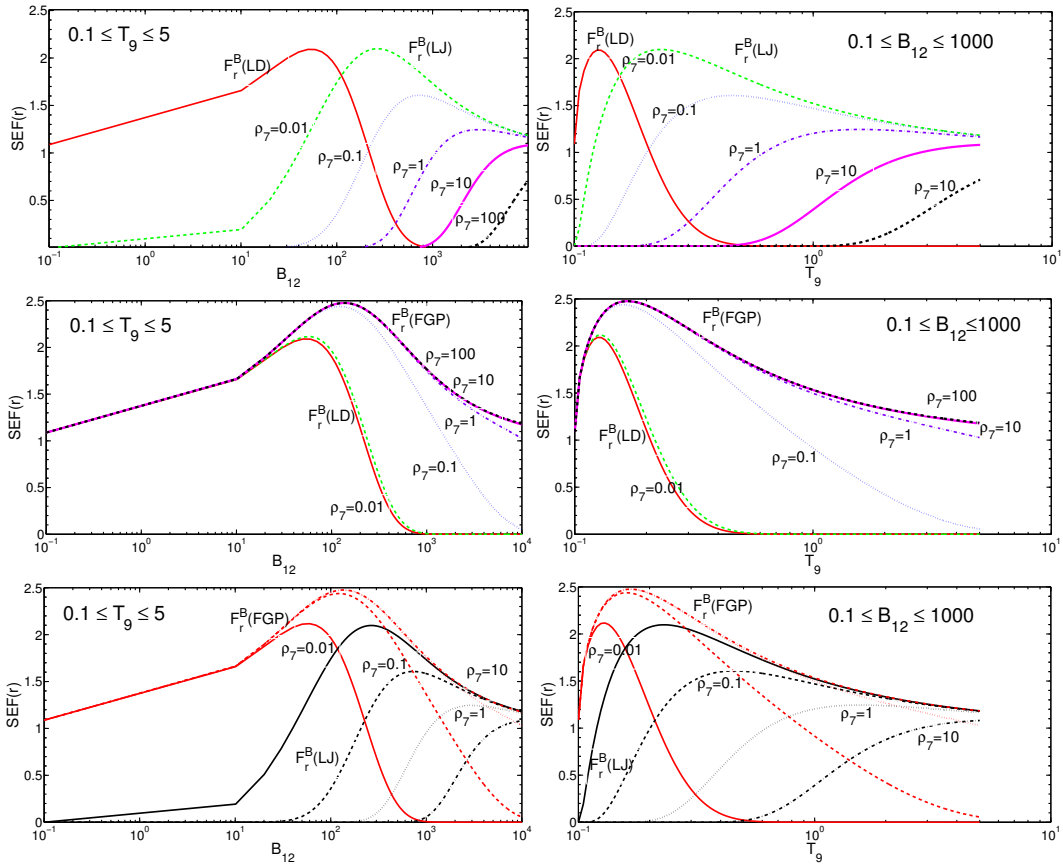

Fig. 5. (color online) Comparisons of the resonant SEF for the LJ, LD, and FGP models, in the case with SES and SMF, for some typical astronomical conditions.

1.66 for $B_{12}=84.18$ and $\rho_7=0.01$. However, the SEF increases with increasing B_{12} at relatively high density (e.g. $\rho_7=1$), then reaches a maximum value of 5.166 at $T_9=0.2$. Sub-figures 4(c) and 4(d) show that in the LJ model the SEF increases with increasing B_{12}, and reaches a maximum at 5.056 for $B_{12}=1000$, $T_9=0.2$ and $\rho_7=0.01$.

In Figure 5, the resonant SEF is compared for the LJ, LD, and FGP models for typical astronomical conditions in a SMF. The results of the LD model agree well

with those of the FGP model for relatively low density (e.g., $\rho_7 \leqslant 0.01$). However, the SEF of our model decreases smoothly with increasing B_{12} and T_9, until it is comparable with those of LD and FGP.

The SES problem always plays an important role in stellar evolution. Based on a statistical mechanical theory for the screening function, Dewitt et al. [16] investigated the influence of electron screening on nuclear reactions. Based on a mean-field model, Liolios et al. [17] also studied the effect of screened nuclear reactions. However, they neglected the influence of SMFs on SES. We compare the SEF of these two models (Dewitt and Liolios models) with those of LD, FGP, and LJ. We conclude that the SEF of the Dewitt model is larger than that of the other three SES models for $B_{12}<140$, $\rho_7=0.01$ and $T_9<0.17$, as shown in Fig. 6. However, when $T_9<0.18$, $\rho_7=0.01$, the results of our model are larger than those of Dewitt and Liolios. At a relatively high density (e.g., $\rho_7=0.1$), the SEFs of the LD, FGP and LJ models decrease due to SMFs and are lower than that of the Dewitt model. The results obtained by Ref. [16] amount to an overestimation of the screening effect because they neglect the spatial dependence of the screening function.

Table 1 shows the SEF for the five typical models under some astronomical conditions. The results of LD, FGP, and LJ are always lower than those of Liolios and Dewitt, due to the SMF. The SEF of our model decreases greatly with increasing density and temperature when $B_{12}=10^3$. This is because the ESP increases very rapidly as the SMF increases. The higher the ESP, the larger the influence on SES becomes. On the other hand, the SEF of LD decreases with increasing magnetic field because ESP is reduced. The SEF of the FGP model reaches a maximum of 1.929 when $B_{12}=10^3, \rho_7=1, T_9=0.5$ and then decreases slowly as the density and temperature increase.

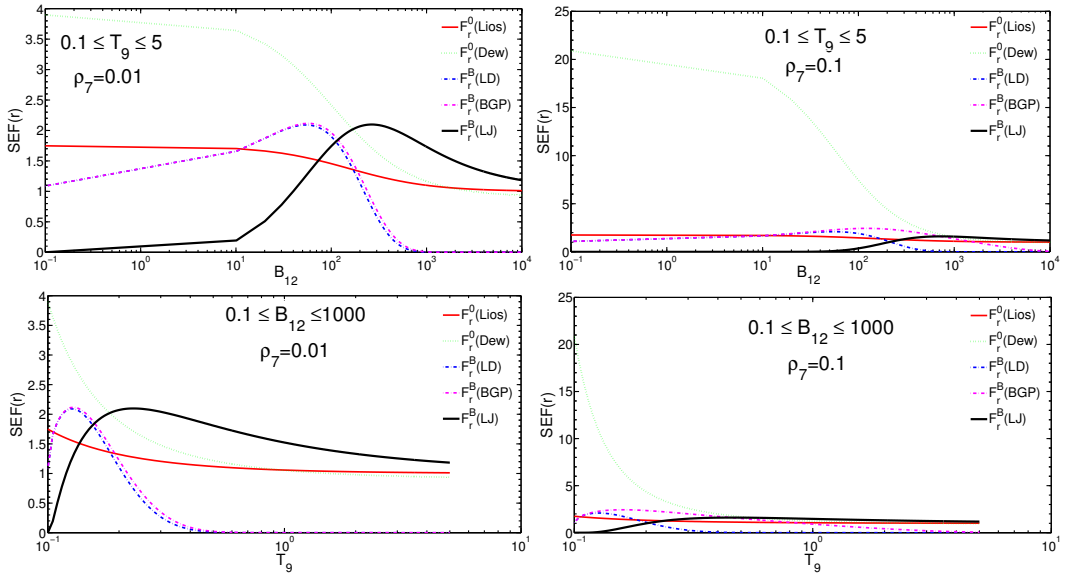

Fig. 6. (color online) Comparisons of the resonant SEF for the Liolios and Dewitt models with those of the LD, FGP, and LJ models.

Table 1. Comparisons of the resonant SEFs for Dewitt, Liolios, LD, FGP and LJ models in several typical astronomical conditions. The former two models do not include SES and SMFs, while the latter three models do include SES and SMFs.

ρ_7	T_9	F_r^0(Lios)	F_r^0(Dew)	$B_{12}=10$			$B_{12}=10^3$		
				F_r^B(LD)	F_r^B(FGP)	F_r^B(LJ)	F_r^B(LD)	F_r^B(FGP)	F_r^B(LJ)
0.01	0.1	1.7475	3.8973	1.6956	1.6964	0.1749	1.0725e-15	1.3472e-13	25.5680
0.05	0.1	1.7475	10.9451	1.6956	1.7013	8.4513e-4	1.0725e-15	0.6045	19.5717
0.1	0.2	1.3219	4.3605	1.3021	1.3045	0.0022	3.2750e-8	2.4894	3.8848
0.1	0.3	1.2051	2.5873	1.1922	1.1941	0.0174	1.0221e-5	1.8371	2.4713
0.2	0.3	1.2045	3.3934	1.1924	1.1939	9.1604e-4	1.0236e-5	2.4990	2.1361
0.3	0.4	1.1497	2.8170	1.1411	1.1422	7.7822e-4	1.8097e-4	2.1178	1.6055
1.0	0.5	1.1181	3.5124	1.1113	1.1122	6.2630e-7	0.0011	1.9290	0.9512
10	0.7	1.0830	7.2692	1.0780	1.0791	6.2012e-9	0.0072	1.6142	0.0894

The Thomas-Fermi screening wave-number $K_{\rm TF}$ is a key parameter which strongly depends on the electron number density and ESP. In consequence, the electron number density and ESP will play important roles in a SMF. Lai et al. [29] analyzed in detail the electron Fermi energy and electron number density in a SMF based on the works of Canuto et al. [41, 42], Kubo. [43], and Pathria [44]. By using the uniform electron gas model and linear response theory, Lai [27] discussed the electron energy (per cell) corrections due to non-uniformity in a SMF. According to their theory, we study the ESP and the SES model (i.e., LD model). The results show that the ESP decreases as the magnetic fields increase due to the diminution of electron chemical potential. The LD model is valid only in the condition of $K_{\rm TF}{\rm r}_i \ll 1$ at lower densities, because they investigated the non-uniformity effect only through detailed electronic (band) structure calculations.

The electron chemical potential is a pivotal parameter, which is closely related to the electron number density and exchange energy. Based on the Thomas-Fermi-Dirac approximation, it is given as [30]

$$U_{\rm F}=U_{\rm e}=\frac{\partial w_{\rm ex}}{\partial n_{\rm e}}=\frac{r_{\rm cyc}}{\pi a_0}\hbar\omega_0 nI(n), \tag{48}$$

where $w_{\rm ex}$ is the exchange energy and $I(n)$ can be found in Ref. [30]. By using the linear response theory, Fushiki et al. [30] discussed the exchange energy and electron chemical potential in the lowest Landau level for non-uniform electron gas in a SMF. They analyzed the SES problem in a SMF and their results showed that in a SMF only the lowest Landau level is occupied by electrons on the condition of $r_{\rm e} > (3\pi/8)^{1/3}r_{\rm cyc}$ or equivalently $\rho < 7.04\times10^3 B_{12}^{3/2}({\rm A/z}){\rm g/cm^3}$. The cyclotron radius in the lowest Landau level orbital is give by $r_{\rm cyc}=(2\hbar c/eB)^{1/2}\simeq 3.36\times10^{-10}B_{12}^{-1/2}$. FGP used the expression of $n_{\rm e}\partial n_{\rm e}/\partial U_{\rm F}=(3/2)n_{\rm e}/U_{\rm F}$ in dealing with $\partial n_{\rm e}/\partial U_{\rm F}$. In the FGP model, they thought that at high density the exchange correction is very small, thus they neglected the exchange correction to $\partial n_{\rm e}/\partial U_{\rm F}$ and had $n_{\rm e}\partial n_{\rm e}/\partial U_{\rm F}=(1/2)n_{\rm e}/U_{\rm F}$ in a SMF. Due to different ways of dealing with exchange correction under this condition, the SEF of the FGP model has some differences compared with other SES models.

According to statistical physics the microscopic state number ${\rm d}x{\rm d}y{\rm d}z{\rm d}p_x{\rm d}p_y{\rm d}p_z$ can be given by ${\rm d}x{\rm d}y{\rm d}z{\rm d}p_x{\rm d}p_y{\rm d}p_z/h^3$ in a 6-dimensional phase-space. The number of states occupied by completely degenerate relativistic electrons per volume is calculated by [41, 42]

$$\begin{aligned} N_{\rm phase} &= \sum_{p_x}\sum_{p_y}\sum_{p_z}=\frac{1}{h^3}\int_{-\infty}^{\infty}\int_{-\infty}^{\infty}\int_{-\infty}^{\infty}{\rm d}p_x{\rm d}p_y{\rm d}p_z \\ &= \frac{1}{h^3}\int_0^{p_{\rm F}}{\rm d}p_z\int_0^{\infty}p_\perp{\rm d}p_\perp\int_0^{2\pi}{\rm d}\theta=\frac{\pi p_{\rm F}}{h^3}\int_0^{\infty}{\rm d}p_\perp^2, \end{aligned} \tag{49}$$

where $\theta = tan^{-1}p_y/p_x$, $p_\perp^2\to m^2c^4\frac{B}{B_{\rm cr}}2n$, So, $\int_0^\infty {\rm d}p_\perp^2\to\sum_{n=0}^\infty\omega_n$, where ω_n is the degeneracy of the n-th electron Landau level in a relativistic magnetic field, and can be calculated by [42–44]

$$\begin{aligned} \omega_n &= \frac{1}{h^2}\int_0^{2\pi}{\rm d}\phi\int_{k_1<p_\perp^2<k_2}p_\perp{\rm d}p_\perp=\frac{2\pi}{h^2}\frac{(k_2-k_1)}{2} \\ &= \frac{1}{2\pi}\left(\frac{\hbar}{m_ec}\right)^{-2}\frac{B}{B_{\rm cr}}=\frac{b}{2\pi}\left(\frac{\hbar}{m_ec}\right)^{-2}, \end{aligned} \tag{50}$$

where $k_1=2nm_{\rm e}^2c^2\frac{B}{B_{\rm cr}}=2nbm_{\rm e}^2c^2$, and $k_2=2(n+1)bm_{\rm e}^2c^2$.

Based on the works of Peng et al. [20], Gao et al. [22], which introduced the Dirac δ-function and considered the Pauli exclusion principle, we have discussed the SES problem in a SMF. Our results show that the stronger the magnetic field, the higher the Fermi energy of the electrons becomes. The ESP increases with SMF and the maximum value of ESP is 0.1 MeV in a SMF. The SEF also increases greatly and its maximum approaches 5.0 MeV (e.g. $\rho_7=0.01, T_9=0.2, B_{12}=10^3$ G).

4.2 Investigation of nuclear reaction rates

In explosive hydrogen-burning stellar environments, the nuclear reaction $^{23}{\rm Mg(p,\gamma)^{24}Al}$ plays a key role because of breaking out of the Ne-Na cycle to heavy nuclear species (i.e., the Mg-Al cycle). Therefore, it is very important to accurately determine the rates for the reaction $^{23}{\rm Mg(p,\gamma)^{24}Al}$. However, the resonance energy has a large uncertainty due to the inconsistent $^{24}{\rm Mg(^3He,t)^{24}Al}$ measurements mentioned. This may lead to a factor of 5 variation in the reaction rate at $T_9 = 0.25$ because of its exponential dependence on $E_{\rm r}$ [5]. Some authors have discussed the contributions from several important resonance states, including Refs. [1, 3, 5, 45]. To reduce the uncertainty of the reaction rates in this paper, we reference some information about this reaction; the values of $E_{{\rm r}_i}, E_{\rm x}$ and corresponding $\omega\gamma_i$, and some average values of $\omega\gamma_i$, are adopted and listed in Table 2. Based on this data, we analyse the total rates for the five SES models.

Tables 3 and 4 give a brief description of the factor S_i (i = 1,2,3) for the LD, FGP, and LJ models when $B_{12}=10$ and 10^3. As the density and temperature increase, the results of the LD model are in good agreement with those of FGP, but disagree with our results at $B_{12}=10$. This is because the electron Fermi energy of our model is lower than those of LD and FGP in relatively low magnetic fields. As the magnetic fields increase from $B_{12}=10$ to 10^3, the factor S_3 increases by about 2$\sim$3 orders magnitude (i.e., from 0.1749 to 25.5680 and from 0.0022 to 3.8848) when $\rho_7=0.01, T_9=0.1$ and $\rho_7=0.1, T_9=0.2$, respectively. When $B_{12}=10^3$ the factor S_3 is about 39.74, 5.69, 1.56 times larger than S_2 (FGP model) at $\rho_7=0.03, T_9=0.2$, $\rho_7=0.05, T_9=0.2$

and $\rho_7=0.1, T_9=0.2$, respectively. From what has been discussed above, the LD model is perhaps only suitable for a relatively low magnetic field and low density environment. The FGP and LD models are both unsuited to relatively low density and high magnetic field surroundings (e.g. $\rho_7<0.1, B_{12}>10^2$). However, our model is well suited to relatively high magnetic field and low density surroundings (e.g. $B_{12}>10^2, \rho_7<0.05$).

Summing up the above discussion, our calculations show that this SES effect in a SMF can increase nuclear reaction rates of ^{23}Mg (p,γ)^{24}Al by several orders magnitude. More precise thermonuclear rates of ^{23}Mg (p,γ)^{24}Al will help us to constrain the determination of nuclear flow out of the Ne-Na cycle, and production of $A \geq 20$ nuclides, in explosive hydrogen burning over a temperature range of $0.2 \leq T \leq 1.0$ GK.

Table 2. Resonance parameters for the reaction ^{23}Mg (p,γ) ^{24} Al.

E_x/MeV[a)]	E_x/MeV[b)]	J^π	E_{r_i}/MeV[c)]	Γ_p	Γ_γ	$\omega\gamma_i$/meV[d)]	$\omega\gamma_i$/meV[e)]	$\omega\gamma_i$/meV[f)]
2.349±0.020	2.346±0.000	3^+	0.478	185	33	25	27	26
2.534±0.013	2.524±0.002	4^+	0.663	2.5e3	53	58	130	94
2.810±0.020	2.792±0.004	2^+	0.939	9.5e5	83	52	11	31.5
2.900±0.020	2.874±0.002	3^+	1.029	3.4e4	14	12	16	14

a) is adopted from Ref. [46]; b) from Ref. [5]; c) from Ref. [47]; d) from Ref. [4]; e) from Ref. [45]; f) is adopted in this paper

Table 3. Comparison of the rates of λ_r^0, without SES, with those of the LD (λ_r^{scB}(LD)), FGP (λ_r^{scB}(FGP)) and our calculations λ_r^{scB}(LJ), with SES, for some typical astronomical conditions at $B_{12}=10$. $S_i=\lambda_{ri}^{scB}/\lambda_r^0$, i=1,2,3 denote the rates of LD, FGP, and LJ model, respectively.

ρ_7	T_9	λ_r^0	$B_{12}=10$			S_1	S_2	S_3
			λ_r^{scB}(LD)	λ_r^{scB}(FGP)	λ_r^{scB}(LJ)			
0.01	0.1	1.0942e-19	1.8552e-19	1.8561e-19	1.9138e-20	1.6956	1.6964	0.1749
0.02	0.1	1.0942e-19	1.8552e-19	1.8598e-19	4.0569e-21	1.6956	1.6998	0.0371
0.03	0.1	1.0942e-19	1.8552e-19	1.8608e-19	1.0413e-21	1.6956	1.7007	0.0095
0.03	0.2	4.2967e-8	5.5949e-8	5.6034e-8	4.1916e-9	1.3021	1.3041	0.0976
0.04	0.2	4.2967e-8	5.5949e-8	5.6041e-8	2.2448e-9	1.3021	1.3043	0.0522
0.05	0.2	4.2967e-8	5.5949e-8	5.6044e-8	1.2491e-9	1.3021	1.3043	0.0291
0.1	0.2	4.2967e-8	5.5949e-8	5.6051e-8	9.3383e-11	1.3021	1.3045	0.0022
0.2	0.4	0.0163	0.0186	0.0186	8.5713e-5	1.1411	1.1422	0.0053
0.3	0.5	0.1925	0.2140	0.2141	6.2713e-4	1.1114	1.1122	0.0033
0.5	0.6	0.9764	1.0663	1.0669	8.5404e-4	1.0920	1.0927	8.7465e-4
0.7	0.8	7.2550	7.7500	7.7537	0.0079	1.0682	1.0687	0.0011
1.0	0.9	14.0604	14.9100	14.9162	0.0050	1.0604	1.0609	3.5785e-4

Table 4. Comparison of the rates of λ_r^0, without SES and SMFs, with those of the LD (λ_r^{scB}(LD)), FGP (λ_r^{scB}(FGP)) and our calculations λ_r^{scB}(LJ), with SES, for some typical astronomical conditions at $B_{12}=10^3$. $S_i=\lambda_{ri}^{scB}/\lambda_r^0$, i=1,2,3 denote the rates of LD, FGP, and LJ model, respectively.

ρ_7	T_9	λ_r^0	$B_{12}=10^3$			S_1	S_2	S_3
			λ_r^{scB}(LD)	λ_r^{scB}(FGP)	λ_r^{scB}(LJ)			
0.01	0.1	1.0942e-19	1.1735e-34	1.4740e-32	2.7975e-18	1.0725e-15	1.3472e-13	25.5680
0.02	0.1	1.0942e-19	1.1735e-34	6.4612e-24	2.5883e-18	1.0725e-15	5.9052e-5	23.6555
0.03	0.1	1.0942e-19	1.1735e-34	1.5306e-21	2.4177e-18	1.0725e-15	0.0140	22.0969
0.03	0.2	4.2967e-8	1.4072e-15	5.0819e-9	2.0198e-7	3.2750e-8	0.1183	4.7007
0.04	0.2	4.2967e-8	1.4072e-15	1.7120e-8	1.9575e-7	3.2750e-8	0.3984	4.5559
0.05	0.2	4.2967e-8	1.4072e-15	3.3408e-8	1.9009e-7	3.2750e-8	0.7775	4.4240
0.1	0.2	4.2967e-8	1.4072e-15	1.0696e-7	1.6692e-7	3.2750e-8	2.4894	3.8848
0.2	0.4	0.0163	2.9459e-6	0.0324	0.0288	1.8097e-4	1.9876	1.7669
0.3	0.5	0.1925	1.9523e-4	0.3509	0.2812	0.0010	1.8227	1.4604
0.5	0.6	0.9764	0.0031	1.6579	1.1949	0.0032	1.6979	1.2237
0.7	0.8	7.2550	0.0976	10.8789	7.8159	0.0135	1.4995	1.0773
1.0	0.9	14.0604	0.3053	20.2526	13.6742	0.0217	1.4404	0.9725

5 Conclusions

In this paper, based on relativistic theory in a SMF, we have investigated the problem of SES, and the SES influence on the nuclear reaction of ^{23}Mg (p,γ)^{24}Al by LD, FGP, and LJ strong screening models in a SMF. The results show that the SES thermonuclear reaction rates have a remarkable increase in a SMF. The rates can increase by around three orders of magnitude. For example, when B_{12} increases from 10 to 10^3, the rates increase from 0.1749 to 25.5680 at ρ_7=0.01,T_9=0.1, and from 0.0022 to 3.8848 at $\rho_7=0.1$,$T_9=0.2$. The considerable increase in the reaction rates for ^{23}Mg (p,γ) ^{24}Al implies that more ^{23}Mg will escape the Ne-Na cycle due to SES in a SMF. Then it will make the next reaction convert more ^{24}Al (β^+,ν) ^{24}Mg to participate in the Mg-Al cycle. It may lead to synthesis of a large amount of heavy elements at the crust of magnetars. These heavy elements, which are produced from the nucleosynthesis process, may be thrown out due to the compact binary mergers of double neutron star (NS-NS) or black hole and neutron star (BH and NS) systems. Furthermore, our model for the rates is in good agreement with those of the LD and FGP models at relatively low density (e.g., $\rho_7<0.01$) and $B_{12}<10^2$. In relatively low magnetic fields (e.g., $B_{12}<1$), the SES of the LD and FGP models have a strong influence on the rates compared to our model. However, the rates in our model can be about 1.58 times and three orders of magnitude higher than those of FGP and LD, respectively, in relatively high magnetic fields and low density surroundings (e.g., $B_{12}\geqslant10^2$, $\rho_7<0.05$). The results we derived may have very important implications in some astrophysical applications for nuclear reactions, thermal evolution, and numerical simulation of magnetars.

We would like to thank the anonymous referee for carefully reading the manuscript and providing some constructive suggestions which were very helpful to improve this manuscript.

References

1 R. K. Wallace and S. E. Woosley, ApJS., **45**: 389 (1981)
2 C. Iliadis, J. M. D'Auria, S. Starrfield et al, ApJS, **134**: 151 (2001)
3 S. Kubono, T. Kajino, and S. Kato, Nucl. Phys. A., **588**: 521(1995)
4 H. Herndl, M. Fantini, C. Iliadis, P. M. Endt, and H. Oberhummer, Phys. Rev. C., **58**: 1798 (1998)
5 D. W. Visser, C. Wrede, J. A. Caggiano et al, Phys. Rev. C., **76**: 5803 (2007)
6 J. J. Liu and D. M. Liu, RAA, 2017, arXiv:1711.01955
7 J. N. Bahcall, L. Brown, A. Gruzinov, and R. Sawer, AandA, **383**: 291 (2002)
8 J. J. Liu, MNRAS, **433**: 1108 (2013)
9 J. J. Liu, MNRAS, **438**: 930 (2014)
10 J. J. Liu, RAA, **16**: 83 (2016)
11 J. J. Liu et al, RAA, **17**: 107 (2017)
12 J. J. Liu et al, ChPhC, **41**: 095101 (2017)
13 E. E. Salpeter and H. M. van Horn, ApJ, **155**: 183 (1969)
14 E. E. Salpeter, AuJPh., **7**: 373 (1954)
15 H. C. Graboske and H. E. DeWitt, ApJ, **181**: 457 (1973)
16 H. E. Dewitt, Phys. Rev. A., **14**: 1290 (1976)
17 T. E. Liolios, EPJA., **9**: 287 (2000)
18 T. E. Liolios, Phys. Rev. C., **64**: 8801 (2001)
19 Z. F. Gao et al, ChPhB, **21**: 057109 (2012)
20 Q. H. Peng and H. Tong, MNRAS, **378**: 159 (2007)
21 Z. F. Gao., N. Wang, J. P. Yuan, L. Jiang, and D. L. Song, ApandSS, **332**: 129(2011)
22 Z. F. Gao, N. Wang, Q. H. Peng, X. D. Li, and Y. J. Du, Mod. Phys. Lett. A., **28**: 50138 (2013)
23 Z. F. Gao., N. Wang, Y. Xu, H. Shan, and X. D. Li., AN, **336**: 866(2015)
24 Z. F. Gao., N. Wang, H. Shan, X. D. Li, and W. Wang, ApJ, eprint arXiv:1709.03459
25 Z. F. Gao., Y. Xu, H. Shan, X. D. Li., H. Shan, W. Wang, and N. Wang., AN, eprint arXiv:1709.02186 (2017)
26 X. H. Li, Z. F. Gao, X. D. li et al, IJMPD, **25**: 1650002(2016)
27 D. Lai, Rev. Mod. Phys., **73**: 629 (2001)
28 R. C. Duncan and C. Thompson, ApJ, **392**: 9 (1992)
29 D. Lai and S. L. Shapiro, ApJ, **383**: 745 (1991)
30 I. Fushiki, E. H. Gudmundsson, and C. J. Pethick, ApJ, **342**: 958 (1989)
31 L. D. Landau and E. M. Lifshitiz, *Quantium mechanics*, (3rd ed., Oxford: Pergamon Press 1977), p.457
32 C. Zhu, Z. F. Gao., X. D. Li et al, Mod. Phys. Lett. A., **31**: 50070(2016)
33 N. W. Ashcroft and N. D. Mermin, *Solid State Physics*, (Saunders College: Philadelphia 1976), p.123
34 B. B. Kadomtsev and O. P. Pogutse, Phys. Rev. L., **25**: 1155 (1971)
35 J. M. Lattimer, C. J. Pethick, D. G. Ravenhall, and D. Q. Lamb, Nucl. Phys. A., **432**: 646 (1985)
36 W. Stolzmann and T. Bloecker, AandA, **314**: 1024 (1996)
37 D. G. Yakovlev and D. A. Shalybkov, Astrophys. Space. Phys. Rev., **7**: 311 (1989)
38 W. A. Fowler, G. R. Caughlan, and B. A. Zimmerman, ARAandA., **5**: 525 (1967)
39 A. M. Lane and R. G. Thomas, Rev. Mod. Phys., **30**: 257 (1958)
40 H. Schatz, A. Aprahamian, J. Goerres et al, Phys. Rep., **294**: 167 (1998)
41 Canuto, V. and H. Y. Chiu, Phys. Rev., **173**: 1210 (1968)
42 Canuto, V. and H. Y. Chiu, Space. Sci. Rev., **12**: 3 (1971)
43 R. Kubo, *Statistics Mechanics*, (Amsterdam: North-Holland Publishing Co.1965) p.278
44 R. K. Pathria, *Statistics Mechanics*, (2nd. Singapore: Isevier 2003), p.280
45 M. Wiescher, J. Gorres, F.-K. Thielemann, and H. Ritter, AandA, **160**: 56 (1986)
46 P. M. Endt, Nucl. Phys. A., **633**: 1 (1998)
47 G. Audi and A. H. Wapstra, Nucl. Phys. A., **595**: 409 (1995)